ENGINEERING

Chemical recycling of mixed textile waste

Erha Andini[1,2], Pooja Bhalode[3], Evan Gantert[1], Sunitha Sadula[3]*, Dionisios G. Vlachos[1,2,3]*

Globally, less than 0.5% of postconsumer textile waste is recycled, with the majority incinerated or ending up in landfills. Most postconsumer textiles are mixed fibers, complicating mechanical recycling due to material blends and contaminants. Here, we demonstrate the chemical conversion of postconsumer mixed textile waste using microwave-assisted glycolysis over a ZnO catalyst followed by solvent dissolution. This approach electrifies the process heat while allowing rapid depolymerization of polyester and spandex to their monomers in 15 minutes. A simple solvent dissolution enables the separation of cotton and nylon. We assess the quality of all components through extensive material characterization, discuss their potential for sustainable recycling, and provide a techno-economic analysis of the economic feasibility of the process.

INTRODUCTION

The increasing global population and wealth have increased the demand for fiber production, with 113 million tons of global fiber produced in 2021 and 149 million tons projected by 2030 if business continues as usual (*1*–*3*). The rising demand for textiles and shorter life span compared to a generation ago due to fast fashion result in a substantial accumulation of waste, estimated to be 92 million tons globally yearly (*2*–*5*). Less than 1% of textile waste is recycled, with approximately 73% dumped in landfills or incinerated, 14% lost during production and collection, and 12% downcycled into lower-value applications (*6*, *7*). This results in a notable loss of valuable resources and substantial environmental issues.

Mechanical recycling is the most used method due to its simplicity and low cost (*8*, *9*). Yet, it cannot handle multifiber textiles, additives, or colorants. It shortens the fiber length (*10*–*12*) and decreases its quality to lower-value products, such as insulation material, mattress stuffing, and wiping cloths (*5*). The most widely used textile fibers consist of poly(ethylene terephthalate) (PET) polyester, the same material as in PET bottles, whose market share was 54% of the global fiber production in 2021 (*1*). While PET chemical recycling techniques, such as hydrolysis, methanolysis, glycolysis, and enzymatic depolymerization, have extensively been studied, the polyester is often interlaced tightly with other fibers (synthetic or natural polymers) consisting of cotton, nylon, spandex, dyes, and finishes. Mixed textile waste requires costly sorting and separation before reprocessing to avoid an undesirable mixture of products (*13*, *14*). A three-step procedure to recycle polyester from mixed textile waste to purified and decolorized bis(2-hydroxyethyl) terephthalate (BHET) has been reported (*8*) using a homogeneous catalyst, high temperatures, and long reaction times for decolorization and glycolysis without addressing the remaining unreacted solids. This compositional complexity requires direct recycling or upcycling to convert mixed textile waste efficiently. To our knowledge, no reports on chemical recycling of complex textile waste that account for the fate of all components exist.

Here, we demonstrate a strategy to handle the polyester, cotton, nylon, and spandex in real postconsumer mixed textile waste in short reaction times (15 min) under microwave (MW)–assisted glycolysis over a ZnO catalyst. We completely degrade polyester and spandex into their monomers while producing intact cotton and nylon (Fig. 1). The impact of textile dyes and finishes is discussed. The potential array of products from each component and their market values are considered. Last, economic viability of our process is explored. This study provides new insights into the chemical recycling of mixed textile waste. Further refinement of this process holds the potential to achieve a global textile circularity rate of 88%.

RESULTS AND DISCUSSION

Feedstock characterization

We started with a well-defined feedstock of white 100% polyester textile, white 100% cotton textile, and white 50/50 blend of polyester and cotton T-shirt, referred to hereafter as 50/50 PolyCotton. These feedstocks were chosen due to the polyester and cotton dominance in the fiber market, holding 54 and 22% share, respectively (*1*). The known compositions set benchmark standards for complex mixtures whose composition varies. Thermogravimetric analysis (TGA), Fourier transform infrared (FTIR), differential scanning calorimetry (DSC), x-ray diffraction (XRD), and scanning electron microscopy (SEM) provide insights into the distinct morphological and thermal characteristics of polyester and cotton textiles (*15*–*18*); see the "Feedstock characterization" section in the Supplementary Materials.

Polyester depolymerization in the presence of cotton

Earth-abundant metal oxides, such as ZnO, are attractive catalysts due to their robustness, low cost, high activity, and ease of separation and recycling (*19*–*22*). We have recently reported complete depolymerization of singe-stream PET pellets and plastic bottles in ethylene glycol (EG) under MW-assisted heating using a ZnO catalyst (*19*). Glycolysis produces BHET, the esterification product of terephthalic acid with EG, which can be recycled directly, eliminating the extra esterification step.

We performed glycolysis of white 100% polyester and 100% cotton textiles (Fig. 2) under the optimized reaction conditions of our previous work (*19*), demonstrating excellent activity on the polyester textile despite morphology differences from PET pellets, with 99% conversion and 90% yield of BHET. The cotton experienced a 7.8% mass loss upon glycolysis. The FTIR spectra of cotton's solid residue (fig. S4) resemble that of 100% cotton, indicating that cotton does not participate in glycolysis. Blank experiments of 100% cotton with and

[1]Department of Chemical and Biomolecular Engineering, University of Delaware, 150 Academy St., Newark, DE 19716, USA. [2]Catalysis Center for Energy Innovation, University of Delaware, 221 Academy St., Newark, DE 19716, USA. [3]Center for Plastics Innovation, 221 Academy St., Newark, DE 19716, USA.
*Corresponding author. Email: sunithak@udel.edu (S.S.); vlachos@udel.edu (D.G.V.)

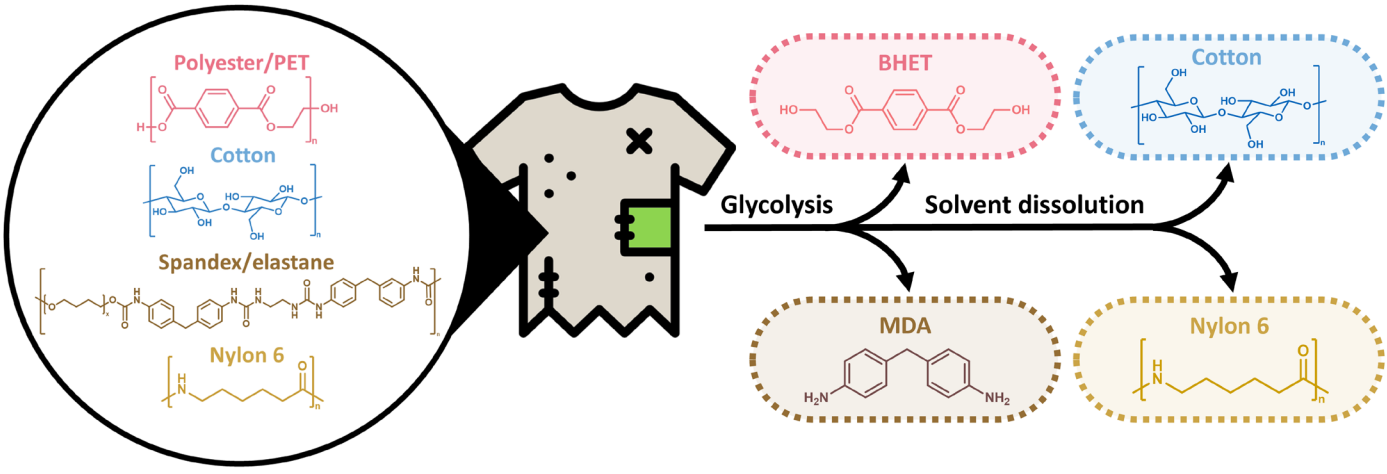

Fig. 1. Overview of the chemical full recycling process. Conversion of real mixed textile waste (polyester, cotton, spandex, and nylon) using MW-assisted glycolysis and solvent dissolution. BHET, bis(2-hydroxyethyl) terephthalate; MDA, 4,4′-methylenedianiline.

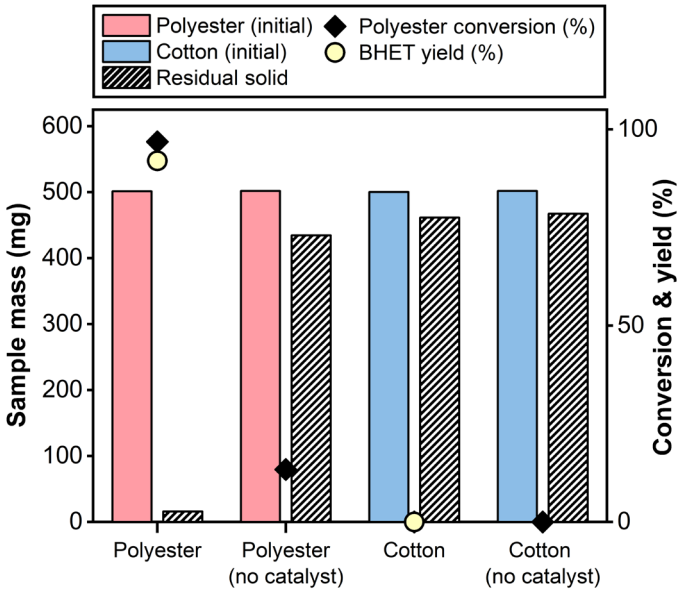

Fig. 2. Glycolysis of pure textiles. Conversion of 100% polyester and 100% cotton textiles after MW-assisted depolymerization with and without catalyst. Reaction conditions are as follows: 0.5 g of textile, 5 mg of ZnO, 5 ml of EG, 210°C, and 45 min.

without a catalyst confirm that moisture loss (~5%) and light cotton degradation upon prolonged heating rather than catalyst activity are responsible for this mass loss (table S1) (*23*).

Using the 50/50 PolyCotton T-shirt, we performed time-dependent experiments at various temperatures to understand the effect of cotton on polyester glycolysis when the two are interlaced tightly. Only the polyester reacts while the cotton remains intact. Higher temperatures notably accelerate the complete depolymerization of the polyester (Fig. 3) (*19*, *20*). The cotton does not participate in the glycolysis chemistry (*24*, *25*). The color of the solution upon glycolysis changes from light yellow hue at 150°C after 15 min to dark orange hue at 210°C after 45 min (Fig. 3, B to D). This coloration occurs due to the gradual decomposition of cotton upon prolonged heating at elevated temperatures (*26*).

At 150°C, the conversion increases at short times and then evolves slowly due to the slow depolymerization of polyester (16) and the cotton swelling by the solvent (24), which hinders mixing. At 180°C, the conversion keeps increasing up to 30 min, whereas at 210°C, complete polyester conversion is achieved in less than 15 min. The BHET yield data traces, in general, the conversion data. The more notable difference between the two at lower temperatures is attributed to forming intermediate polyester oligomers, indicating that depolymerization involves internal C—O bond scission several units apart rather than unzipping the backbone to monomers. At longer times, these oligomers convert to monomers. This hypothesis is supported by a powder seen on the dried remaining solids, indicative of oligomers (Fig. 3E) (*20*, *27*). Such powders are absent in the dried remaining solids at 210°C after 15 min.

To confirm the complete conversion of polyester at 210°C after 15 min, the solid residue was characterized. TGA data in Fig. 4A show that upon glycolysis, the characteristic polyester peak disappeared, and the curve resembles that of cotton. Similarly, the XRD and FTIR spectra upon glycolysis (Fig. 4, B and C) resemble that of cotton alone (highlighted in light gray). A slight decrease in the crystallinity of the recovered cotton on the XRD spectra suggests that the glycolysis chemistry affects the crystal morphology of cotton (*15*, *28*). The small peak on the solid residue at ~1550 cm^{-1} in the FTIR spectra corresponds to the leftover EG solvent. The findings are further corroborated by SEM, where only convoluted cotton fibers are observed (Fig. 4D and fig. S5).

The effect of dyes and finishes on polyester depolymerization

We performed catalytic glycolysis on commercial textile materials, addressing a diverse range of textile waste with potential unidentifiable dyes, additives, and impurities. These textiles, featuring various dyes (red, blue, and yellow) and standard finishes [antimicrobial, antistatic, ultraviolet (UV) resistant, fire resistant, and water stain resistant], underwent glycolysis without pretreatment, as shown in Fig. 5. The color-coded bars reflect the textiles' actual colors. Our emphasis

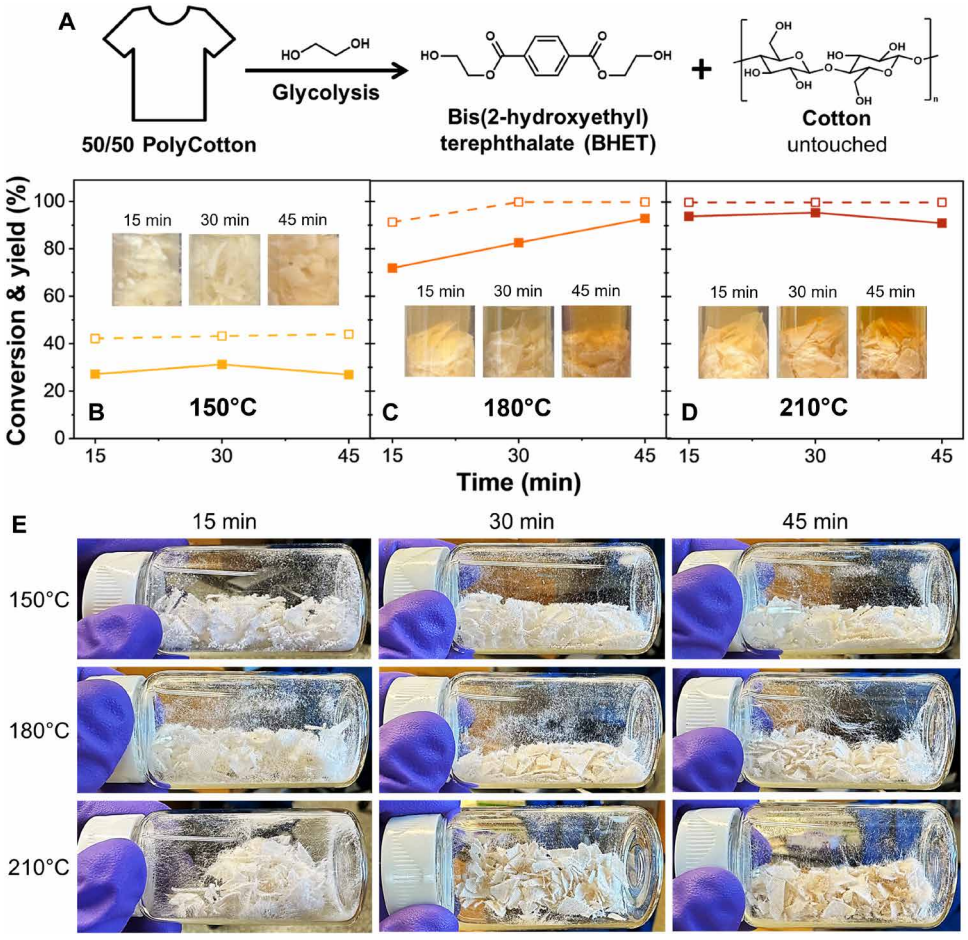

Fig. 3. Glycolysis results of interlaced polyester and cotton (50/50 PolyCotton). (**A**) Schematic of deconstruction process. Conversion of polyester (points connected by dashed lines) and yield of BHET (points connected by solid lines) as a function of time at (**B**) 150°C, (**C**) 180°C, and (**D**) 210°C. Reaction conditions are as follows: 0.5 g of textile (50/50 PolyCotton T-shirt), 5 mg of ZnO, and 5 ml of EG. (**E**) Solid residues upon glycolysis at temperatures and times indicated.

centered on red, blue, and yellow textiles because they represent the three primary colors. Finish classification relied on information provided by retail store labels.

The BHET yield for dyed textiles was lower than for undyed (white) polyester textiles. Disperse dyes, exclusively suitable for polyester, bond to fibers through van der Waals forces and hydrogen bonding (*29*) and appear to interact with and hinder the catalyst activity (*30*). The blue textile dyes have a less profound effect due to their bulkier nature that causes steric hindrance or pore inaccessibility, resulting in a higher BHET yield (plausible structures are shown in fig. S6). This implies a need for longer reaction times for colored textiles, which could affect scalability and economic feasibility.

Notably, the glycolysis product solution is rich in dyes, indicating the potential for recycling (*8*, *31*, *32*). Textiles with antimicrobial, antistatic, and water- and stain-resistant finishes exhibited similar trends. UV- and fire-resistant finishes negatively affected glycolysis. The former increased textile hydrophobicity, causing mixing challenges with the hydrophilic EG solvent. The low yield for a fire-resistant finish is attributed to phosphorus (table S2), leading to char formation. Phosphorus compounds can physically and chemically deactivate catalysts and substrates (*33*–*35*), highlighting the need for further research into optimizing glycolysis conditions for textiles with such finishes.

The precise dyes and finishes in commercial textiles are challenging to determine due to the diversity in dye molecules and complex formulations. Understanding the implications of these complexities is crucial for developing sustainable solutions for textile waste management and advancing circular economy principles.

The effect of textiles size reduction on glycolysis

Cotton fibers longer than half an inch (≥13 mm) can be reused in spinning yarn (*3*). The effectiveness of fiber-to-fiber recycling in cotton textiles centers on preserving the length or degree of polymerization (DP) inherent in naturally produced cotton. This preservation is attainable through mechanical carding instead of shredding. We used two flat wooden paddles with wire teeth for carding, separating the 50/50 PolyCotton into individual fibers. Figure 6 (A and B) depicts the distinct morphologies of the textiles and the consequential impact on glycolysis chemistry. We observed a substantial difference in absorbency between shredded 50/50 PolyCotton and carded 50/50 PolyCotton fibers at room temperature. With their increased surface area and exposed–OH functionality, carded fibers absorbed the solvent more, as depicted in Fig. 6C. Yet, dispersing the solvent and catalyst, even with vortexing, proved challenging, resulting in incomplete polyester depolymerization into BHET, with unreacted fibers and

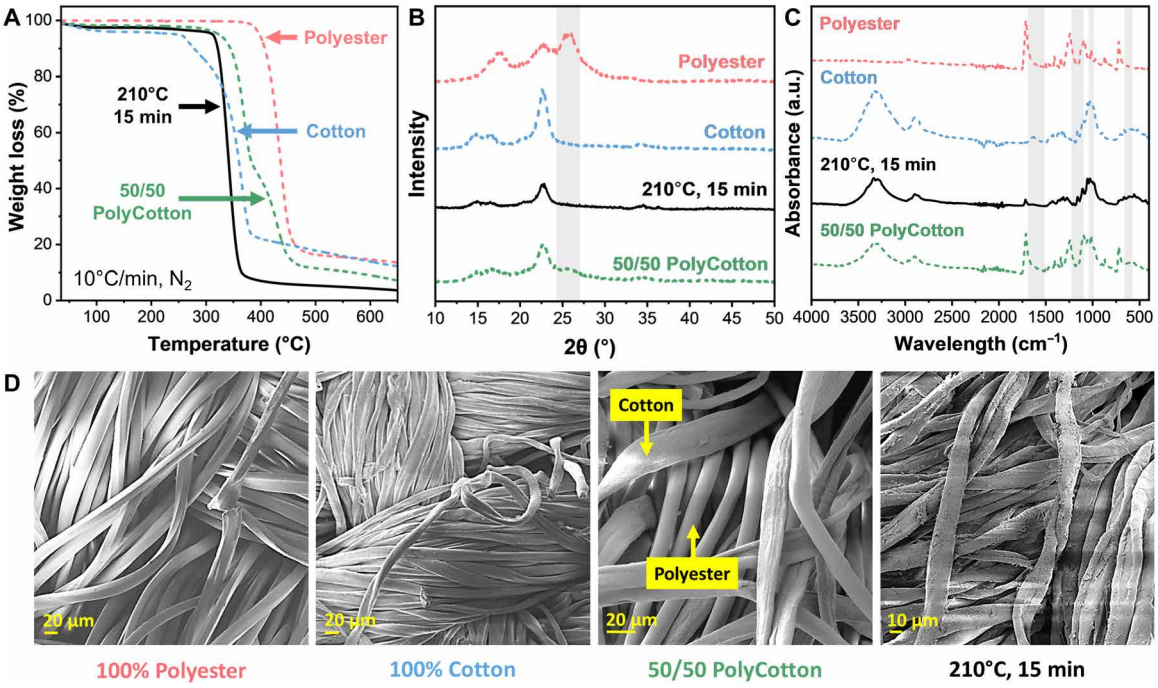

Fig. 4. Characterization of residual solid. (**A**) TGA, (**B**) XRD, (**C**) FTIR, and (**D**) SEM patterns of solid residue (solid black lines) upon glycolysis of 50/50 PolyCotton compared to initial 100% polyester (pink dashed lines), 100% cotton (blue dashed lines), and 50/50 PolyCotton (green dashed lines). a.u., arbitrary units.

oligomers clumps (Fig. 6A). This indicates that the morphology of the textiles is crucial to the conversion and that the distribution of EG is essential for MW-assisted glycolysis. Therefore, while carding effectively preserves the length of cotton fibers, it introduces limitations in mass transfer.

Glycolysis of mixture consisting of polyester, cotton, nylon, and spandex

While polyester and cotton fibers are by far the dominant fibers in textile products, they are often blended with other fibers, with spandex (or elastane) and nylon (or polyamide 6) being prominent. The increasing popularity of activewear and athleisure, along with the growing demand for stretchable fabrics in the apparel and textile sectors, has fueled the demand for spandex and nylon fibers (*36*, *37*). Research on recycling combined polyester, cotton, nylon, and spandex textiles is limited, as most previous studies have focused on dual-material textiles, such as polyester-cotton, cotton-nylon, cotton-elastane, and nylon-elastane blends. When multifiber textile waste has been considered, the emphasis has primarily been on recovering the monomer with no information on the fate of cotton, nylon, and spandex (*8*, *38*).

Initially, we conducted glycolysis of white 100% nylon (N) and 90% nylon/10% spandex (NS) to explore the potential codepolymerization of nylon and spandex during glycolysis. A textile composed entirely of 100% spandex does not exist, resembling more of a rubber band. As shown in Fig. 7, both textiles transformed into powder and sticky solids (fig. S7), experiencing a mass decrease of 15% for N and 13% for NS textiles. FTIR spectra of N's solid residue (fig. S8A) resemble that of the starting textile, indicating no reactivity in glycolysis. Blank experiments with and without a catalyst (fig. S9) confirmed that the mass loss resulted from thermal degradation at 210°C, surpassing the melting temperature of spandex (~170°C) and approximately matching the melting temperature of nylon (~220°C) (*9*, *39*). This degradation is attributed to the degradation of spandex into sticky solids containing polytetrahydrofuran diols (spandex chain extender), melting into the filter paper upon air-drying overnight at 70°C (fig. S10), and diphenylmethane-containing molecules (fig. S14) (*40*, *41*). TGA and DSC results (fig. S8E) of the recovered nylon show shifts to the left after glycolysis. This suggests a reduction in nylon's molecular weight. We suspect that the decomposition products are high molecular weight oligomers and/or caprolactam monomers (9) due to peaks and changes in the number average molecular weight seen on high-performance liquid chromatography (HPLC), liquid chromatography–mass spectrometry (LC-MS), and gel permeation chromatography (GPC) (fig. S8, B to D). However, further studies are required to characterize the exact products.

To confirm whether nylon and spandex affected polyester depolymerization, glycolysis was performed on a blend of white polyester and cotton textiles mixed with N and NS textiles (PCN and PCNS in Fig. 7). The observed mass loss was attributed to the complete depolymerization of polyester and the full and partial degradation of spandex and nylon, as observed earlier. Our results indicate that the other components do not hinder the polyester depolymerization.

Recycling of real textile waste with unknown compositions

The properties of textiles are often tailored for specific applications by incorporating various additives during manufacturing, adding complexity to the deconstruction of discarded textiles with blended compositions. We developed a chemical recycling pathway for real mixed textile waste (Fig. 8) from the University of Delaware Department of Fashion and Apparel Studies. Glycolysis was performed on a shredded random blend (0.5 g in total) with unknown polyester, cotton, nylon, and spandex compositions. At a reaction temperature of 210°C,

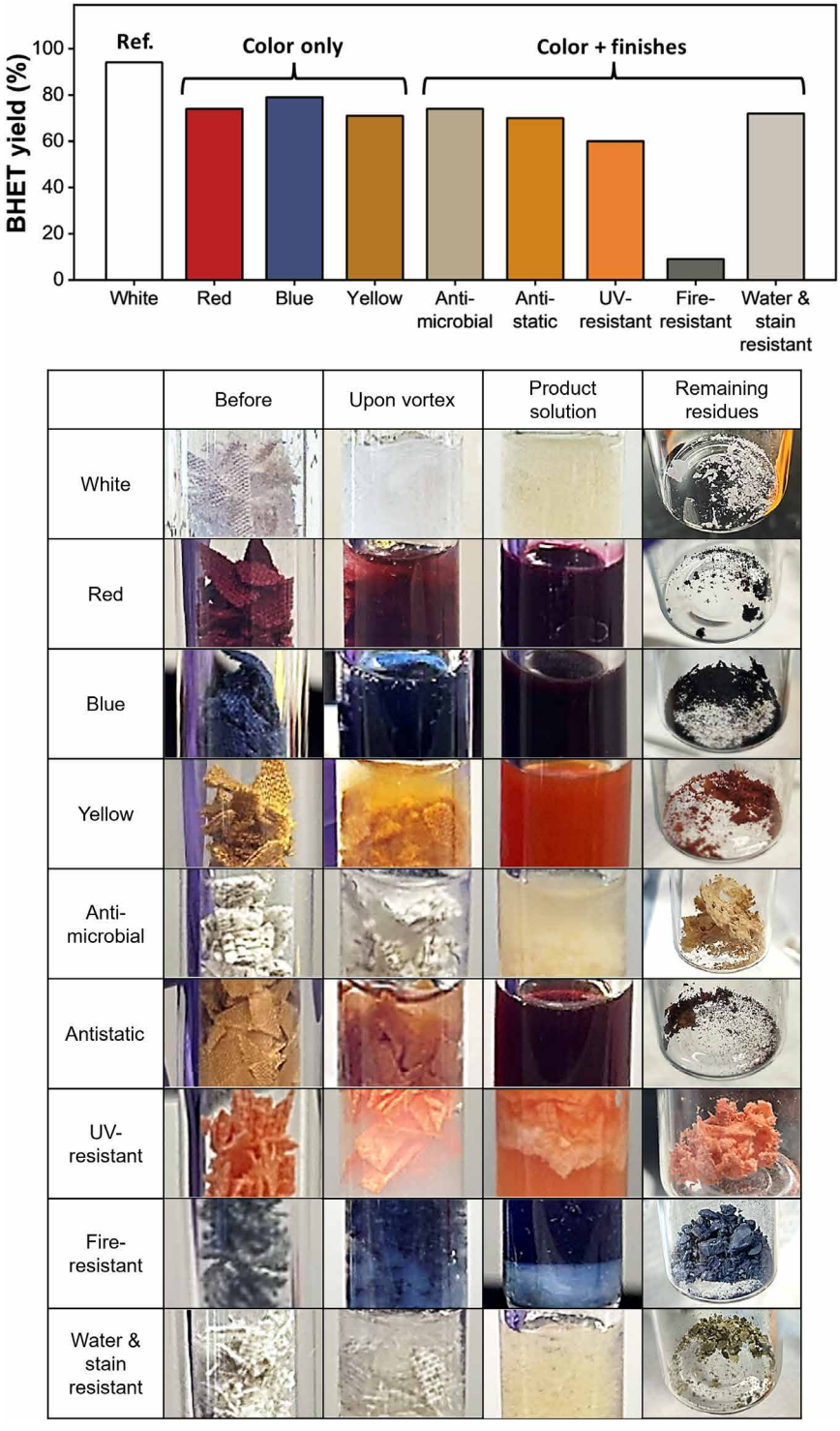

Fig. 5. Glycolysis of polyester textiles in the presence of dyes and finishes. Top: BHET yield from 100% textiles with dyes and finishes. **Bottom**: Solid residues of 100% polyester textiles with dyes and finishes. Reaction conditions are as follows: 0.5 g of 100% polyester textile, 5 mg of ZnO, 5 ml of EG, 210°C, and 15 min.

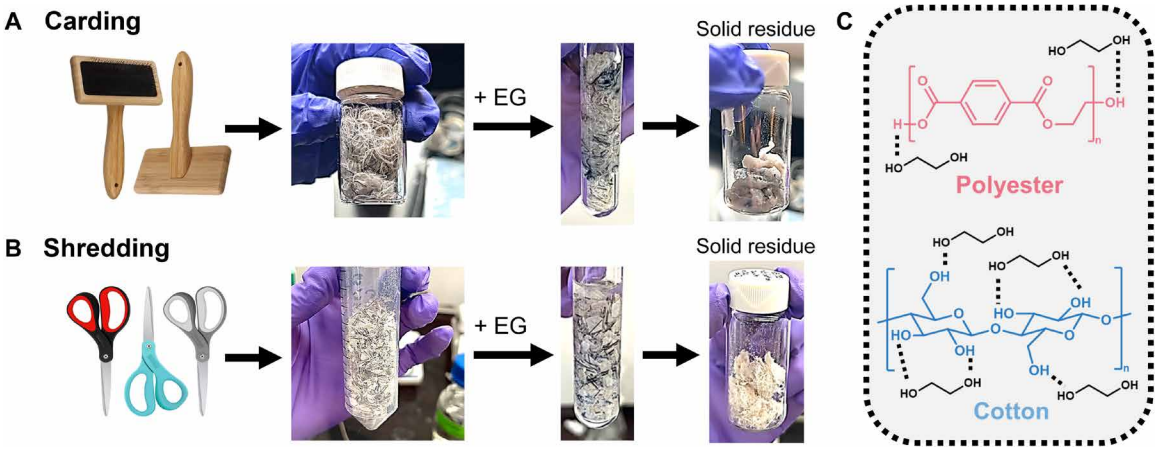

Fig. 6. Effect of textiles morphology. Carding (**A**) versus shredding (**B**) and hydrogen bonding between polymers and solvent (**C**).

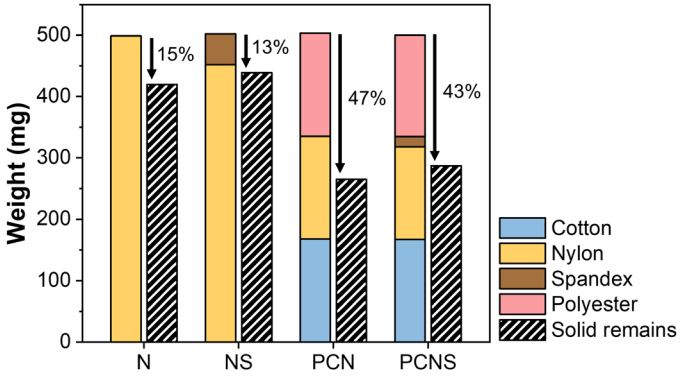

Fig. 7. Glycolysis of polyester, cotton, nylon, and spandex. Reaction conditions are as follows: 0.5 g of textile, 5 mg of ZnO, 5 ml of EG, 210°C, and 45 min. Left bar indicates the composition of each feedstock, and right bar indicates the residual solid for each case. *N* = 100%. Nylon (NS), 90% nylon and 10% spandex; PCN, 100% polyester:100% cotton:100% nylon (1:1:1); PCNS, 100% polyester:100% cotton:90% nylon and 10% spandex (1:1:1).

polyester was completely converted to BHET, and spandex was transformed into diphenylmethane-containing molecules and sticky polyols (spandex chain extender). Cotton and nylon remained intact.

To recover BHET crystals, the product solution—now primarily containing BHET, EG, and water—underwent vacuum distillation to remove the water. This process leaves behind the EG fraction, which still contains BHET. The residual EG fraction was cooled overnight to 4°C in a refrigerator, forming BHET crystals. These crystals were simply filtered and dried at 80°C. The BHET, isolated through crystallization, underwent characterization by nuclear magnetic resonance (NMR), TGA, and DSC (fig. S12). Additional peaks, likely from decomposed dyes or organic impurities, are indicated in the recovery of nonwhite BHET crystals with 93% purity (fig. S13). Complete BHET decolorization can be achieved through subsequent recrystallization (*42*). The remaining EG contains the diphenylmethane-containing molecules from spandex (confirmed by LC-MS, as seen in fig. S14) and a mixture of unknown dyes implicated by the brown EG solution (Fig. 8A). Among all the diphenylmethane-containing molecules obtained, 4,4′-methylenedianiline (MDA) was found to be the most valuable (*40*). MDA can be isolated using techniques such as solvent extraction, precipitation, or column chromatography (*9*, *38*, *40*). Further optimization is needed to increase the selectivity of MDA from the other diphenyl-containing molecules.

Unreacted cotton, nylon, and polyols (spandex chain extender) are insoluble in EG and were easily filtered off. Washing the remaining solids with deionized water and air-drying them overnight at 100°C resulted in the degraded polyols melting into the filter paper and separating from the cotton and nylon. Nylon and cotton were separated through simple solvent dissolution using 90% formic acid at room temperature. Nylon is hard to solubilize because of the strong hydrogen bond interaction between the amide groups. According to American Society for Testing and Materials (ASTM) D629, 90% formic acid is the only known solvent that solubilizes nylon at room temperature while keeping cotton intact (*43*). We observed that the dissolution of nylon occurred instantly upon contact with formic acid due to protonation of the carbonyl bonds by formic acid, disrupting the hydrogen bonding between the amide group within nylon chains but not strong enough to cause cotton degradation (*44*). The dissolved nylon was simply filtered off from cotton. The cotton was further washed with water and air-dried overnight at 70°C. Nylon was recovered by distilling out the formic acid. The isolated cotton and nylon were characterized by TGA, FTIR, DSC, and XRD (figs. S15 and S16). Some formic acid and dyes remained in the isolated cotton. Complete removal of formic acid can be achieved through subsequent washing with methanol and water. The remaining dyes, likely covalently bonded to cotton fibers, proved more challenging to remove (*29*). Solvent dissolution and distillation for nylon recovery substantially reduced its crystallinity (fig. S16D). The decrease in recovered nylon's number average molecular weight compared to 100% nylon textile without treatment (fig. S16E) is likely due to the reaction treatment at elevated temperatures.

The mixed textile waste offers the potential for making multiple products (Table 1). The recovered BHET can be directly repolymerized into polyester (*45*), with a market value ranging from $1.1 to $2.7/kg, depending on application (*46*–*49*). The polyester obtained presents a clear entry point for the yarn making of textiles through melt spinning (*50*). MDA, a high-value monomer used in various

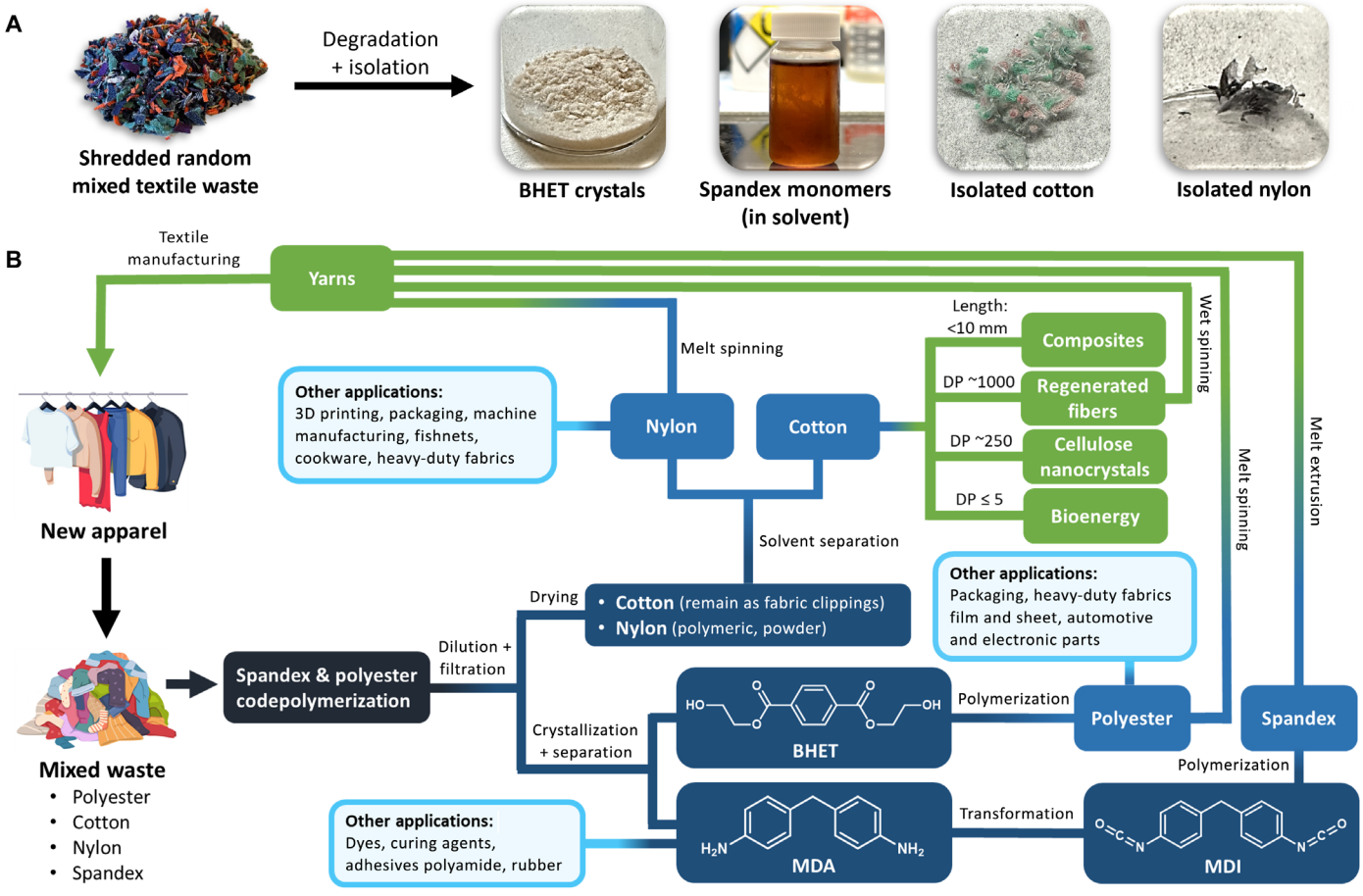

Fig. 8. Recycling of mixed textile waste for circularity. (**A**) Isolated components obtained from real mixed textile waste with unknown compositions. (**B**) Proposed pathways for textile-to-textile and open-loop recycling. 3D, three-dimensional. MDI, methylene diphenyl diisocyanate.

industries, has a market value ranging from $2.5 to $100/kg (*51*–*55*). MDA can be reintroduced into textile production by chemically transforming it into methylene diphenyl diisocyanate (MDI), followed by polymerization with polyols to create recycled spandex (*50*). Successful fiber-to-fiber cotton recycling relies on preserving a high DP in cellulose (9000 to 15,000). However, multiple home laundering cycles lead to the aging of cotton fibers (*56*). Cutting and shredding the textile waste before chemical degradation result in fiber damage and breakage. All these result in a lower DP value of postconsumer cotton textile waste than virgin cotton. If used as is to make yarns, then the durability and strength of the yarns will be low (*57*). Alternatively, the short cotton fibers produced can be blended with virgin cotton to improve the quality of recycled yarn and reduce the cost of virgin yarn raw materials. They can also be used in composites to make regenerated fibers (e.g., viscose and lyocell) and cellulose nanocrystals or as fermentation feedstock for energy applications (*3*, *58*, *59*). The market values range from $2.2 to $5.0/kg and $0.1/kWh for bioenergy (*48*, *60*, *61*). The recovered nylon can be melted and turned back into yarns or used in automotive, food, industrial, and composite applications. Its market value ranges from $2.5 to $50/kg (*53*, *55*, *62*–*64*). However, the reduced molecular weight could limit its applications for uses that require high tensile strength, stiffness, and melting point. The actual prices of all these applications vary based on region and material quality. Figure 8B directly illustrates the potential for transforming mixed textile waste, regardless of its composition, back into textiles or for open-loop recycling.

In our process, dyes and changes in properties might hinder the use of recovered BHET, MDA, cotton, and nylon in various applications. To address this, additional steps are necessary. BHET can be decolorized using activated carbon after redissolving in fresh EG at 100°C for 3 hours through subsequent recrystallization in EG, yielding white BHET at ≥99% purity (fig. S13). Adjusting processing conditions during manufacturing can enhance nylon's crystallinity (*65*), influencing its mechanical properties and processing methods. Nylon, like BHET, can be decolorized using activated carbon after dissolution in formic acid at 100°C for a longer time due to the high concentration of dyes. However, the inevitable reduction in recovered nylon's molecular weight compared to 100% nylon textile limits its use in various applications. Thus, further research is needed to determine the optimal processing conditions for decoloring and minimizing reduction in molecular weight or achieve full deconstruction. The remaining reactive dyes and the inevitable reduced DP of end-of-life cotton textiles diminish the value of the recovered cotton, requiring

Table 1. Textile waste product map, harnessing its compositional complexity. FRP, Fiberglass-reinforced plastic; MDA, 4,4′-methylenedianiline.

Products	Category	Applications	Value ($/kg)
Polyester (from BHET)	Yarn	Garments, sportswear, jackets, coats, rainwear, suits, dresses, curtains, drapes, tablecloths, bedspreads, and other home furnishing products	2.7
	Filament	Ropes, cords, and fishing nets	1.1
	Resin	Boats, pipes, tanks, helmets, surfboards, coatings, adhesives, and sealants	1.6
Nylon	Yarn	Stretchy apparel such as leggings, socks, shirts, underwear, dresses, and trousers and home décor such as blankets, pillows	4.2
	Automotive	Tires, airbags, and seat belts	4.1
	Food	Food packaging and strainers	2.5
	Industrial	3D printing, ropes, cords, and fishing nets	2.6–50
	Composite	FRP products such as boats, pipes, tanks, and helmets	4.0
Cotton	Yarn	Garments, sportswear, jackets, coats, rainwear, suits, dresses, curtains, drapes, tablecloths, bedspreads, and other home furnishing products	5.0
	Composites	Automotive, construction, and packaging	2.2
	Regenerated fibers	Textiles, nonwovens, and hygiene products	4.3
	Bioenergy	Heating, electricity, and transportation	$0.1 kWh
MDA	Polyurethane foams	Insulation, cushioning, and packaging	2.7
	Epoxy resins and adhesives	Glues, paints, inks, dental bonding agents, and microelectronic encapsulations	2.5
	Fiberglass reinforced plastic	Boats, pipes, tanks, and helmets	4.0
	High-performance polymers	Aerospace, electronics, and engineering	12–100

further research on removing reactive dyes and regenerating the fibers beyond the study's scope. The high solubility and low purity of MDA in EG complicate its recovery, highlighting the necessity for efficient methods, such as distillation and extraction. Removing EG through vacuum distillation and using solvent-solvent extraction to separate MDA and other diphenyl-containing molecules from dyes is recommended (fig. S17). Further optimization is required to achieve a high yield of MDA recovery from mixed textile waste and simplify the process.

Because of the unknown starting material composition, determining precise conversion and yield is challenging. Nevertheless, in the broader context of global fiber production (52% polyester, 24% cotton, 6% man-made cellulosic fiber, 5% nylon, and 1% spandex) (*1*), refining this process further holds the potential to achieve a textile circularity rate of 88%. The presented methodology demonstrates efficacy in managing complex mixed textile waste, simulating real-world conditions of unsorted textile waste disposed in landfills. Sorting such waste is recognized as a time-consuming and costly endeavor. The process can recover all components, but further improvements will be necessary.

Techno-economic assessment

To assess the economic feasibility, we conducted a techno-economic analysis (TEA) of the process outlined in Fig. 8. We created a process flowsheet using Advanced System for Process Engineering (ASPEN) Plus, followed by TEA evaluation, as shown in Fig. 9. We specifically focused on a textile feed throughput of 500 kg/hour. We considered a case with low product sales and another with high product sales, as detailed in Table 1. This deliberate approach allowed us to understand how varying product sales affect economic viability.

Our analysis used the profitability index (PI) as a key metric. For cases 1 and 2, we obtained PIs of 0.95 and 1.29, respectively, with a value of 1 indicating breakeven. The costs outlined in Table 1 include capital ($6.5 million), operating ($92 million), and raw material

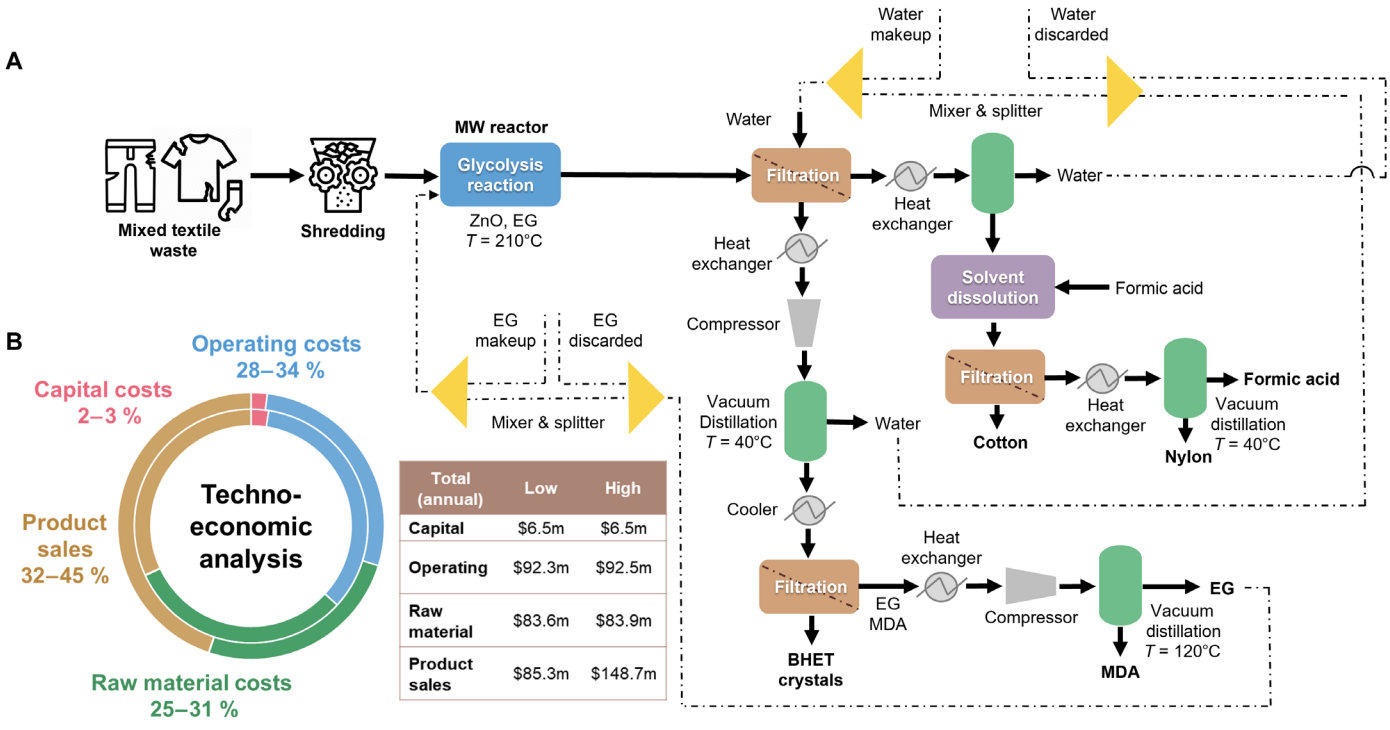

Total (annual)	Low	High
Capital	$6.5m	$6.5m
Operating	$92.3m	$92.5m
Raw material	$83.6m	$83.9m
Product sales	$85.3m	$148.7m

Fig. 9. Techno-economic analysis of the proposed process. (**A**) Process developed in ASPEN. (**B**) Cost breakdown for TEA analysis including capital, operating, raw material costs, and product sales. Here, the inner and outer circles correspond to TEA results with lower and higher margins of product stream sales.

($84 million) with product sales, amounting to $85.4 million for case 1 and $148.7 million for case 2.

These findings highlight the intricate relationship between product sales and project viability. In addition, our analysis suggests that as processing capacities increase, leveraging economies of scale, profit margins, and the project's overall economic feasibility improve. This insight underscores the significance of scalability and strategic planning in maximizing the proposed approach's economic potential.

Previously, our group has shown that MW-assisted single stream of polyester recycling for BHET production provided 6.9 times reduction of global warming potential over the traditional petroleum driven pathway (*66*). Given this reduction, MW-assisted BHET production is incorporated in the proposed process as well. Future work will explore the sustainability aspect in detail, incorporating a systematic life cycle assessment for circularity of mixed waste textiles.

In summary, recycling mixed fibers is challenging due to the complex blend of materials and contaminants. Here, we demonstrated a strategy for converting mixed textile waste. By performing individual and mixed component experiments, we found slight interactions among components. This allowed us to achieve complete depolymerization of polyester into BHET and spandex into its monomers, with MDA being the most valuable, in short reaction times (15 min) under MW-assisted heating over ZnO catalyst. Cotton and nylon remain mostly intact. Certain textile dyes and finishes, such as flame retardants, are detrimental to the glycolysis chemistry. Preremoval of these will enable one to obtain colorless components without retarding glycolysis. Some of the recovered components can be integrated directly into the textile and clothing manufacturing value chain for textile-to-textile recycling and the others into different applications. This study provides insights into the chemical-based recycling of mixed textile waste. Further refinement of this process holds the potential to achieve a global textile circularity rate of 88%.

MATERIALS AND METHODS

Chemicals and materials

Control fabrics were purchased from JoAnn, including 100% polyester (white and colored with or without finishes) and 100% cotton (bleached and scoured). The postconsumer textile waste was obtained from Goodwill provided by the University of Delaware Department of Fashion and Apparel Studies. EG (anhydrous, 99.8%), BHET (>98.4%), zinc oxide (<50 nm), and deuterated dimethyl sulfoxide (DMSO-d_6) (99.9%) were obtained from Sigma-Aldrich. Ultrapure (type 1) water was used (Direct-Q 3 UV-R). All textiles and chemicals were used as received.

Reaction procedures

All experiments were performed on a Monowave 450 MW reactor (Anton Paar GmbH). This batch MW reactor controls the temperature, time, and maximum set power. An in-built infrared sensor and an external Ruby thermometer allow temperature control. Typically, 500 mg of textiles, 5 ml of EG, and 5 mg of the catalyst were placed in a MW reaction vial. The vial was inserted into the MW reactor, and the reactor was programmed to maintain a constant temperature. On completion of a reaction, the reaction vial was allowed to cool down rapidly to room temperature. One hundred millilters of distilled water was added to separate BHET and oligomers. The unreacted polymer and larger oligomers were removed using a Whatman filter paper. The filtrate consisting of the products dissolved in water was analyzed using HPLC (see below). The residual water from the product solution

was then evaporated under vacuum (72 mbar) at 60°C using a rotary evaporator, and the resulting BHET was crystallized by cooling the residual solution overnight to 4°C in a refrigerator after the addition of a small amount of distilled water to the residue. The resultant crystals were filtered using a glass filter and dried at 80°C.

HPLC was used to quantify BHET concentrations with an Agilent 1260 Infinity coupled with a UV detector and a Zorbax Eclipse Plus C8 column. The mobile phase contained equal volumes of methanol and ultrapure water at a flow of 0.6 ml/min with an injection volume of 10 µl. A BHET calibration curve was constructed using a commercial standard. Conversions of textiles and yields of BHET were calculated using the following equations

$$\text{Textile Conversion}\,(\%) = \frac{m,\mathrm{i} - m,\mathrm{f}}{m,\mathrm{i}} \times 100\,\%$$

$$\text{BHET Yield}\,(\%) = \frac{mol_{\mathrm{BHET}}}{mol_{\mathrm{PET}}} \times 100\,\%$$

$$mol_{\mathrm{PET}}\,(\%) = \frac{W\mathrm{PET,i}}{MW_{\mathrm{PET-RU}}} \times 100\,\%$$

here, m_i corresponds to the initial mass of textile samples, m_f to the mass of the unreacted textile (obtained via filtration), mol_{BHET} to the BHET moles produced, and mol_{PET} to the initial moles of PET. MW_{PET-RU} is the molecular weight of the PET repeating unit [$MW_{PET-RU} = 192$ unified atomic mass units (u)].

Analysis of textile samples and products

Textile samples and BHET crystals were characterized using a Bruker D8 XRD with Cu Kα radiation (λ = 1.54056 Å) at 40 kV and 40 mA. Elemental composition was measured using wavelength dispersive x-ray fluorescence (XRF) on a Rigaku Supermini 200 machine with a Pd anode. ^{1}H NMR and ^{13}C NMR spectra were recorded with Bruker AVIII400 and AVIII600 spectrometers in a DMSO-d_6 solution. The NMR spectra were analyzed using the MestReNova software. Unknown peaks were identified with an Agilent gas chromatography–mass spectrometer with a DB5 column, LC-MS using Thermo Fisher Scientific Q-extractive Orbitrap, and electrospray ionization mass spectrometry. The attenuated total reflectance-Fourier transform infrared (ATR-FTIR) data were collected using a Nicolet Nexus 640 spectrometer with a Smart Orbit Diamond ATR Accessory by scanning the sample from 400 to 4000 nm. DSC was conducted using a TA instruments Discovery 250 at a heating rate of 10°C/min and cooling rate of 5°C/min using 5 to 10 mg of sample. TGA was carried out using a TA instruments Discovery 5500 at a heating rate of 10°C/min under a N_2 atmosphere. SEM images of the textile samples were recorded on an Auriga 60 microscope (Carl Zeiss NTS GmbH) equipped with a Schottky field emission gun. Before imaging, the samples were deposited on an adhesive carbon tape and sputtered by a DESK IV sputter unit (Denton Vacuum Inc.) equipped with Au/Pd target. GPC was performed using an Agilent Technologies 1260 equipped with a PL–hexafluoroisopropanol (HFIP) gel column and refractive index detector. The mobile phase was HFIP + 10 to 20 mM trifluoroacetic acid, the flow rate was 0.3 ml/min, and the column was held at 40°C. Column calibration was performed with narrow dispersity poly(methyl methacrylate) standards.

Technoeconomic assessment

The process was developed for a textile feed throughput of 500 kg/hour, scaled based on the experimental approach outlined in this work. For evaluating the overall economics, the following assumptions were considered:

1) A grass roots or clear field project type was considered.
2) The total operating hours were 8000 hours/year.
3) A working capital percentage of 5% was assumed.
4) A total of 40% tax rate and 20% interest rate were considered for a 10-year economic life of the project.
5) A linear straight line depreciation method was considered.
6) Operating costs incorporated raw material costs, operating supplies, operating labor charges, maintenance, utilities, overhead costs, and general and administrative expenses.
7) Capital costs incorporated equipment purchase, equipment setting, piping, civil, instrumentation, electrical, insulation, subcontracts, overhead, escalation, and contingency costs.
8) The MW reactor efficiency was taken to be 85%, including absorbed energy yield and conversion of electricity to MW energy, and utility cost for MW reactor was calculated accordingly (*66*).
9) Catalyst cost was taken to be $112/kg (*66*).
10) For economic evaluation, dyes and polyols are not considered in the process.
11) Water and EG were recycled back in the process.

Supplementary Materials

This PDF file includes:

Figs. S1 to S18
Tables S1 to S4
References

REFERENCES AND NOTES

1. Textile Exchange, Preferred Fiber And Materials Market Report 2022; https://textileexchange.org/knowledge-center/reports/materials-market-report-2022/.
2. J. P. Juanga-Labayen, I. V. Labayen, Q. Yuan, A review on textile recycling practices and challenges. *Textiles* **2**, 174–188 (2022).
3. S. Wang, S. Salmon, Progress toward circularity of polyester and cotton textiles. *Sustain. Chem.* **3**, 376–403 (2022).
4. S. Bianchi, F. Bartoli, C. Bruni, C. Fernandez-Avila, L. Rodriguez-Turienzo, J. Mellado-Carretero, D. Spinelli, M.-B. Coltelli, Opportunities and limitations in recycling fossil polymers from textiles. *Macromol* **3**, 120–148 (2023).
5. K. Niinimäki, G. Peters, H. Dahlbo, P. Perry, T. Rissanen, A. Gwilt, The environmental price of fast fashion. *Nat. Rev. Earth Environ.* **1**, 189–200 (2020).
6. Ellen MacArthur Foundation, A New Textiles Economy: Redesigning fashion's future; https://ellenmacarthurfoundation.org/a-new-textiles-economy.
7. McKinsey & Company, Scaling textile recycling in Europe—Turning waste into value; https://mckinsey.com/industries/retail/our-insights/scaling-textile-recycling-in-europe-turning-waste-into-value.
8. Z. Chen, H. Sun, W. Kong, L. Chen, W. Zuo, Closed-loop utilization of polyester in the textile industry. *Green Chem.* **25**, 4429–4437 (2023).
9. M. Arifuzzaman, B. G. Sumpter, Z. Demchuk, C. Do, M. A. Arnould, M. A. Rahman, P. Cao, I. Popovs, R. J. Davis, S. Dai, T. Saito, Selective deconstruction of mixed plastics by a tailored organocatalyst. *Mater. Horiz.* **10**, 3360–3368 (2023).
10. H. Cao, K. Cobb, M. Yatvitskiy, M. Wolfe, H. Shen, Textile and product development from end-of-use cotton apparel: A study to reclaim value from waste. *Sustain.* **14**, 8553 (2022).
11. R. B. Baloyi, O. J. Gbadeyan, B. Sithole, V. Chunilall, Recent advances in recycling technologies for waste textile fabrics: A review. *Text. Res. J.* **94**, 508–529 (2023).
12. B. Mu, Y. Yang, Complete separation of colorants from polymeric materials for cost-effective recycling of waste textiles. *Chem. Eng. J.* **427**, 131570 (2022).
13. B. D. Vogt, K. K. Stokes, S. K. Kumar, Why is recycling of postconsumer plastics so challenging? *ACS Appl. Polym. Mater.* **3**, 4325–4346 (2021).
14. L. Gausas, S. K. Kristensen, H. Sun, A. Ahrens, B. S. Donslund, A. T. Lindhardt, T. Skrydstrup, Catalytic hydrogenation of polyurethanes to base chemicals: From model systems to commercial and end-of-life polyurethane materials. *JACS Au.* **1**, 517–524 (2021).

15. S. Choi, H. M. Choi, Eco-friendly, expeditious depolymerization of PET in the blend fabrics by using a bio-based deep eutectic solvent under microwave irradiation for composition identification. *Fibers Polym.* **20**, 752–759 (2019).
16. K. Phan, S. Ügdüler, L. Harinck, R. Denolf, M. Roosen, G. O'Rourke, D. De Vos, V. Van Speybroeck, K. De Clerck, S. De Meester, Analysing the potential of the selective dissolution of elastane from mixed fiber textile waste. *Resour. Conserv. Recycl.* **191**, 106903 (2023).
17. Y. Yang, S. Sharma, C. Di Bernardo, E. Rossi, R. Lima, F. S. Kamounah, M. Poderyte, K. Enemark-Rasmussen, G. Ciancaleoni, J.-W. Lee, Catalytic fabric recycling: Glycolysis of blended pet with carbon dioxide and ammonia. *ACS Sustain. Chem. Eng.* **11**, 11294–11304 (2023).
18. J. Egan, S. Wang, J. Shen, O. Baars, G. Moxley, S. Salmon, Enzymatic textile fiber separation for sustainable waste processing. *Resour. Environ. Sustain.* **13**, 100118 (2023).
19. E. Selvam, Y. Luo, M. Ierapetritou, R. F. Lobo, D. G. Vlachos, Microwave-assisted depolymerization of PET over heterogeneous catalysts. *Catal. Today* **418**, 114124 (2023).
20. S. Najmi, B. C. Vance, E. Selvam, D. Huang, D. G. Vlachos, Controlling PET oligomers vs monomers via microwave-induced heating and swelling. *Chem. Eng. J.* **471**, 144712 (2023).
21. G. Park, L. Bartolome, K. G. Lee, S. J. Lee, D. H. Kim, T. J. Park, One-step sonochemical synthesis of a graphene oxide-manganese oxide nanocomposite for catalytic glycolysis of poly(ethylene terephthalate). *Nanoscale* **4**, 3879–3885 (2012).
22. M. Imran, D. H. Kim, W. A. Al-Masry, A. Mahmood, A. Hassan, S. Haider, S. M. Ramay, Manganese-, cobalt-, and zinc-based mixed-oxide spinels as novel catalysts for the chemical recycling of poly(ethylene terephthalate) via glycolysis. *Polym. Degrad. Stab.* **98**, 904–915 (2013).
23. A. Palme, A. Peterson, H. de la Motte, H. Theliander, H. Brelid, Development of an efficient route for combined recycling of PET and cotton from mixed fabrics. *Text. Cloth. Sustain.* **3**, 9 (2017).
24. M. A. Glaus, L. R. Van Loon, Degradation of cellulose under alkaline conditions: New insights from a 12 years degradation study. *Environ. Sci. Technol.* **42**, 2906–2911 (2008).
25. A. Peterson, J. Wallinder, J. Bengtsson, A. Idström, M. Bialik, K. Jedvert, H. de la Motte, Chemical recycling of a textile blend from polyester and viscose, part I: Process description, characterization, and utilization of the recycled cellulose. *Sustain.* **14**, 7272 (2022).
26. C. Vigneswaran, M. Ananthasubramanian, P. Kandhavadivu, Eds., *Bioprocessing of Textiles* (WPI Publishing, 2014).
27. A. Stoski, M. F. Viante, C. S. Nunes, E. C. Muniz, M. L. Felsner, C. A. P. Almeida, Oligomer production through glycolysis of poly(ethylene terephthalate): Effects of temperature and water content on reaction extent. *Polym. Int.* **65**, 1024–1030 (2016).
28. A. R. Horrocks, S. C. Anand, Eds., *Handbook of Technical Textiles, Volume 1: Principles, Processes and Types of Dyes* (Woodhead Publishing Limited, 2016).
29. M. Clark, Ed., *Handbook of Textile and Industrial Dyeing, Volume 1: Technical Textile Processes* (Woodhead Publishing Limited, 2011).
30. C. S. Nunes, P. R. Souza, A. R. Freitas, M. J. V. da Silva, F. A. Rosa, E. C. Muniz, Poisoning effects of water and dyes on the [Bmim][BF4] catalysis of poly(ethylene terephthalate) (PET) depolymerization under supercritical ethanol. *Catalysts* **7**, 43 (2017).
31. B. Mu, X. Yu, Y. Shao, L. McBride, H. Hidalgo, Y. Yang, Complete recycling of polymers and dyes from polyester/cotton blended textiles via cost-effective and destruction-minimized dissolution, swelling, precipitation, and separation. *Resour. Conserv. Recycl.* **199**, 107275 (2023).
32. A. R. Abouelela, J. P. Hallett, A. E. J. Firth, O. D. Levers, Dye recycling methods, WIPO Patent Application WO/2022/175559 (2022).
33. K. B. Nam, J. H. Yeo, S. C. Hong, Study of the phosphorus deactivation effect and resistance of vanadium-based catalysts. *Ind. Eng. Chem. Res.* **58**, 18930–18941 (2019).
34. R. F. Ilmasani, D. Yao, P. H. Ho, D. Bernin, D. Creaser, L. Olsson, Deactivation of phosphorus-poisoned Pd/SSZ-13 for the passive adsorption of NOx. *J. Environ. Chem. Eng.* **10**, 107608 (2022).
35. K. Salmeia, S. Gaan, G. Malucelli, Recent advances for flame retardancy of textiles based on phosphorus chemistry. *Polymers* **8**, 319 (2016).
36. Acumen Research and Consulting, Spandex Fiber Market Size—Global Industry, Share, Analysis, Trends and Forecast 2023–2032; https://acumenresearchandconsulting.com.
37. Grand View Research, Nylon Market Size, Share & Trends Analysis Report; https://grandviewresearch.com/industry-analysis/nylon-6-6-market.
38. M. B. Johansen, B. S. Donslund, M. L. Henriksen, S. K. Kristensen, T. Skrydstrup, Selective chemical disassembly of elastane fibres and polyurethane coatings in textiles. *Green Chem.* **25**, 10622–10629 (2023).
39. F. Lv, D. Yao, Y. Wang, C. Wang, P. Zhu, Y. Hong, Recycling of waste nylon 6/spandex blended fabrics by melt processing. *Compos. Part B Eng.* **77**, 232–237 (2015).
40. W. H. Xu, L. Chen, S. Zhang, R. C. Du, X. Liu, S. Xu, Y. Z. Wang, New insights into urethane alcoholysis enable chemical full recycling of blended fabric waste. *Green Chem.* **25**, 245–255 (2022).
41. Y. Yin, D. Yao, C. Wang, Y. Wang, Removal of spandex from nylon/spandex blended fabrics by selective polymer degradation. *Text. Res. J.* **84**, 16–27 (2014).
42. Y. Peng, J. Yang, C. Deng, J. Deng, L. Shen, Y. Fu, Acetolysis of waste polyethylene terephthalate for upcycling and life-cycle assessment study. *Nat. Commun.* **14**, 3249 (2023).
43. American Society for Testing and Materials, Standard Test Methods for Quantitative Analysis of Textiles; https://astm.org/d0629-15.html.
44. S. Anwar, D. Pinkal, W. Zajaczkowski, P. Von Tiedemann, H. S. Dehsari, M. Kumar, T. Lenz, U. Kemmer-Jonas, W. Pisula, M. Wagner, R. Graf, H. Frey, K. Asadi, Solution-processed transparent ferroelectric nylon thin films. *Sci. Adv.* **5**, eaav3489 (2019).
45. C. C. Westover, T. E. Long, Envisioning a BHET economy: Adding value to PET waste. *Sustain. Chem.* **4**, 363–393 (2023).
46. IndexBox, World - Polyethylene in Primary Forms - Market Analysis, Forecast, Size, Trends And Insights; https://indexbox.io/search/polyethylene-in-primary-forms-market/.
47. Textile Beacon, Polyester yarn export price see a sharp jump in two years; https://textilebeacon.com/news/polyester-yarn-export-price-jump/.
48. Textile Beacon, Yarn export from India halves in May 2022 as prices surged; https://textilebeacon.com/news/yarn-export-halves-prices-surged/.
49. Fibre2Fashion, Polyester Yarn and Fiber Market: Trends, Prices & Forecast; https://fibre2fashion.com/market-intelligence/texpro-textile-and-apparel/raw-material-prices/polyester-value-chain.
50. S. J. Kadolph, S. B. Marcketti, *Textiles* (Pearson Education, 2016).
51. Thunder Said Energy, Polyurethanes: What upside in energy transition?; https://thundersaidenergy.com/2023/08/10/polyurethanes-what-upside-in-energy-transition/.
52. Business Analytiq, Epoxy Resin price index; https://businessanalytiq.com/procurementanalytics/index/epoxy-resin-price-index/.
53. D. S. Cousins, Y. Suzuki, R. E. Murray, J. R. Samaniuk, A. P. Stebner, Recycling glass fiber thermoplastic composites from wind turbine blades. *J. Clean. Prod.* **209**, 1252–1263 (2019).
54. All About 3D Printing & Additive Manufacturing, 3D Printer Material Cost of 2023; https://all3dp.com/2/3d-printer-material-cost-the-real-cost-of-3d-printing-materials/.
55. Graphene Flagship, Composites, Bulk Applications and Coatings; https://graphene-flagship.eu/industrialisation/roadmap/composites-bulk-applications-and-coatings/.
56. A. Palme, A. Idström, L. Nordstierna, H. Brelid, Chemical and ultrastructural changes in cotton cellulose induced by laundering and textile use. *Cellul.* **21**, 4681–4691 (2014).
57. B. Wanassi, B. Azzouz, M. Ben Hassen, Value-added waste cotton yarn: Optimization of recycling process and spinning of reclaimed fibers. *Ind. Crops Prod.* **87**, 27–32 (2016).
58. K. Subramanian, M. K. Sarkar, H. Wang, Z. H. Qin, S. S. Chopra, M. Jin, V. Kumar, C. Chen, C. W. Tsang, C. S. K. Lin, An overview of cotton and polyester, and their blended waste textile valorisation to value-added products: A circular economy approach–research trends, opportunities and challenges. *Crit. Rev. Environ. Sci. Technol.* **52**, 3921–3942 (2022).
59. E. Andini, J. Bragger, S. Sadula, D. G. Vlachos, Production of neo acids from biomass-derived monomers. *Green Chem.* **25**, 3493–3502 (2023).
60. Textile Technology, Stable world natural fiber production in 2022; Graphene Flagship, Composites, Bulk Applications and Coatings; https://textiletechnology.net/fibers/news/dnfi-stable-world-natural-fiber-production-in-2022-32691.
61. C. Scarlata, G. Mosey, Feasibility Study of Economics and Performance of Biopower at the Chanute Air Force Base in Rantoul, Illinois (National Renewable Energy Laboratory, 2013).
62. Fibre2Fashion, Nylon value chain prices likely to remain bearish, sentiments weak; https://fibre2fashion.com/news/nylon-news/nylon-value-chain-prices-likely-to-remain-bearish-sentiments-weak-282358-newsdetails.htm.
63. Invista, A closer look at our products and brands; https://invista.com/products-brands.
64. Xometry, 3D Printer Filament: Types, Materials, Uses, and Services; https://xometry.com/resources/3d-printing/3d-printer-filament/.
65. Y. Lyu, J. Wu, H. Zhang, C. M. Ó. Brádaigh, D. Yang, Effects of thermal process conditions on crystallinity and mechanical properties in material extrusion additive manufacturing of discontinuous carbon fibre reinforced polyphenylene sulphide composites. *J. Compos. Mater.* **57**, 3775–3787 (2023).
66. Y. Luo, E. Selvam, D. G. Vlachos, M. Ierapetritou, Economic and environmental benefits of modular microwave-assisted polyethylene terephthalate depolymerization. *ACS Sustain. Chem. Eng.* **11**, 4209–4218 (2023).
67. M. Matusiak, D. Kamińska, Liquid moisture transport in cotton woven fabrics with different weft yarns. *Materials* **15**, 6489 (2022).
68. V. A. Dehabadi, H. J. Buschmann, J. S. Gutmann, Durable press finishing of cotton fabrics: An overview. *Text. Res. J.* **83**, 1974–1995 (2013).
69. S. L. Madorsky, S. Straus, Thermal degradation of polymers at high temperatures. *J. Res. Natl. Bur. Stand. Sect. A Phys. Chem.* **63A**, 261–268 (1959).

Acknowledgments: We are grateful to H. Cao for valuable insights on textile production and recycling. We thank Butler Polymer Research Laboratory and the University of Florida Center for Macromolecular Science and Engineering for use of the gel permeation chromatography in the Polymer Chemistry Characterization Laboratory. **Funding:** This work was supported as part of the Catalysis Center for Energy Innovation, an Energy Frontier Research Center funded

by the US Department of Energy, Office of Science, and Office of Basic Energy Sciences under award number DE-SC0001004. The MW instrumentation was supported by the Department of Energy's Office of Energy Efficiency and Renewable Energy's Advanced Manufacturing Office under award number DE-EE0007888-7.6 and the State of Delaware. This research used instruments in the Advanced Materials Characterization Lab (AMCL), W. M. Keck Center for Advanced Microscopy and Microanalysis, and the Mass Spectrometry Facility at the University of Delaware. The authors used the NMR facilities at the University of Delaware, founded by the Delaware COBRE program, supported by a grant from the National Institute of General Medical Sciences–NIGMS (5 P30 GM110758-02) from the National Institutes of Health. **Author contributions:** E.A., S.S., and D.G.V. conceived the project and designed the experiments. E.A. executed all the experiments. P.B. performed the TEA. E.G. reproduced experiments. E.A., P.B., S.S., and D.G.V. wrote the article. All the authors proofread the manuscript. **Competing interests:** E.A., S.S., and D.G.V. are inventors of a provisional patent filed in the US Patent and Trademark Office on 3 November 2023, as a US Patent Application Serial No.: 63/595,788. The authors declare that they have no other competing interests. **Data and materials availability:** All data needed to evaluate the conclusions in the paper are present in the paper and/or the Supplementary Materials.

Submitted 15 February 2024
Accepted 31 May 2024
Published 3 July 2024
10.1126/sciadv.ado6827